Rip current evidence by hydrodynamic simulations, bathymetric surveys and UAV observation

Guido Benassai[1], Pietro Aucelli[2], Giorgio Budillon[2], Massimo De Stefano[2], Diana Di Luccio[2], Gianluigi Di Paola[2], Raffaele Montella[2], Luigi Mucerino[3], Mario Sica[4], and Micla Pennetta[5]

[1]Department of Engineering, University of Naples Parthenope
[2]Department of Science and Technology, University of Naples Parthenope
[3]Department of Earth, Environment and Life Sciences, University of Genova
[4]Autorità di Bacino Campania Centrale
[5]Department of Earth, Environment and Resources Sciences, University of Naples Federico II

Correspondence to: Guido Benassai (guido.benassai@uniparthenope.it)

Abstract. The prediction of the formation, spacing and location of rip currents is a scientific challenge that can be achieved by means of different complementary methods. In this paper the analysis of numerical and experimental data, including UAV observation, allowed to detect the presence of rip currents and rip channels at the mouth of Sele river, in the Gulf of Salerno, southern Italy. The dataset used to analyze these phenomena consisted of two different bathymetric surveys, a detailed sediment analysis and a set of high-resolution wave numerical simulations, completed with the ones Google Earth™ and UAV observation. The grain size trend analysis and the numerical simulations allowed to identify the rip current system, forced by topographically constrained channels incised on the seabed, which were detected by high resolution bathymetric surveys. The study evidenced that on the coastal area of the Sele mouth grain-size trends are controlled by the contribution of fine sediments, which exhibit suspended transport pathways due to rip currents and longshore currents. The results obtained were confirmed by Google Earth™ and UAV observations in different years.

Keywords: rip-currents, hydrodynamic simulations, transport vectors, UAV observation.

1 Introduction

The rip currents are narrow, intense seaward flowing jets that originate within the surf zone and broaden outside the breaking zone. They are known to be a major hazards to beach users as they are the cause of the majority of fatalities within the beach environment (Drozdzewski et al. (2012); Brander et al. (2013); Brighton et al. (2013); Zhang et al. (2012)). They are most often observed to occur when the waves approach at near normal incidence and when there are alongshore variations in bathymetry with the alongshore sand bar incised by rip channels (Bowen (1969)). These rip channels are quasi-periodic alongshore perturbations in the bathymetry which occur at the observed alongshore spacing O(100m) (MacMahan et al. (2006)). The morphology of the rip current system consists of a feeder channel that is parallel to the shoreline, which converges to a deeper rip channel that is oriented in an approximate shore-normal direction. Wright and Short (1984) use the non-dimensional fall

velocity parameter

$$\Omega = \frac{H}{Tw_s} \tag{1}$$

to classify beach states (from dissipative to reflective). The fall velocity parameter was related to the rip density RD, introduced by Short and Brander (1999) which defines the number of rips per km of beach and is defined by

$$RD = \frac{L_b}{y_r} \tag{2}$$

where L_b is the beach length and y_r is the rip spacing. They argued that the intermediate beach states $(2 \leq \Omega \leq 5)$ are characterized by rip current morphology. The alongshore variation of wave height fuels an alongshore variation in wave-induced momentum flux or radiation stress (Longuet-Higgins and Stewart (1964)), which cross-shore variations are balanced by the hydrostatic pressure gradient, giving rise to wave set-up on the beach. The longitudinal gradient of set-up generates local longshore currents which concentrate and join up to generate an offshore return flow which forms the rip current. Recently, rip currents have been differentiated based on whether they occur on open coast or embayed beaches, and on the dominant controlling forcing mechanism (Castelle et al. (2010)). They can be distinguished in hydrodynamic rips, which exist in absence of any morphological control, being transient in occurrence in space and time; boundary rips, which are dominated by the influence of rigid lateral boundaries; bathymetric rips, which are influenced by morphological variability in the surf zone, being relatively persistent in space and time. These features, which are located between the surf zone and the coastline, can be investigated with UAV, which already provided topographic mapping (Turner et al. (2016)), and recently extended their applicability to the surf zone characterization (Holman et al. (2017)). In this paper we made use of this cost-effective survey method for the detection of some bathymetric rips at the mouth of Sele river, in the Gulf of Salerno. Two different seasonally spaced bathymetric surveys (Pennetta et al. (2011b)) were used to evidence the presence of rip channels and classify the rip currents typology, together with their spacing. Finally, the rip current features were observed through different techniques, that are Google Earth™ products obtained in 2007, 2013 and 2015 and very recent images obtained by a UAV survey. The investigated area is the coastline at the Sele River mouth in the Gulf of Salerno, which was the subject of coastal vulnerability and risk evaluation ((Di Paola et al., 2011, 2014), Benassai et al. (2015)) and of coastal morphodynamics (Pennetta et al. (2011b)). In fact the Sele coastal plain involves numerous properties and infrastructures, and is strongly susceptible to marine and river inundation. This paper is structured as follows: the study area, with its morphological and climatological features, is introduced in section 2. The data and models are described in section 3. Numerical and field results are presented and discussed in section 4. Discussion and conclusion are finally drawn in sections 5, 6 respectively.

2 Study area and wave climate

The study concerns a stretch of the beach which borders seawards the alluvial plain of the Sele River, one of the widest alluvial coastal plains of central-southern Italy. This plain stretches between the high rocky coasts of Amalfi, to the NW, and Cilento promontory to the SE, (Campania) and is limited towards the sea by a narrow sandy beach which extends from NW to SE in

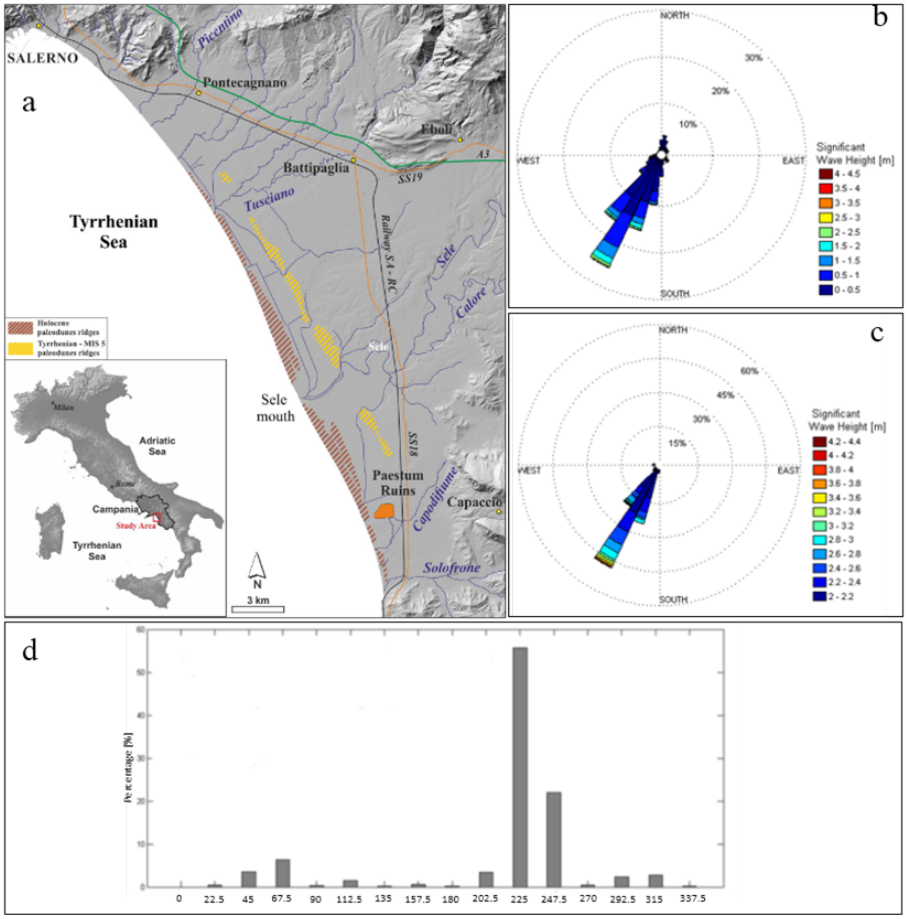

Figure 1. Location map of Coastal Sele Plain (a); directional distribution of the H_s (b) and of the $H_s \geq 2$m recorded by Salerno buoy in the 2014-2016 years (c); H_s occurrence probability [%] for each direction (d).

the Gulf of Salerno, in the southern Tyrrhenian Sea (Fig. 1). The plain represents the emerged portion of a morpho-tectonic depression related to the opening of the Tyrrhenian ocean basin, started during the Upper Miocene (Bartole et al. (1984); Casciello et al. (2006); Aucelli et al. (2012)).

The presence of beach-dune ridges, located in the outer portion of the plain, marks the sea level highstands and Upper Pleistocene paleo-coastlines. During the Holocene, three phases of sandy coastal ridges interrupted the progradational trend of the coastline, with discontinuous dune system height about 3m a.s.l. (Fig. 1a). This dune system can be considered as a natural barrier to sea ingression (e.g. Pennetta et al. (2011a); Pappone et al. (2012); Amato et al. (2013)). Moreover the back-ridge depressions, recently drained, are localized in several and large areas, with a mean elevation of 0.50/1.5m a.s.l. (Pappone et al. (2011)). During the last century, the Sele coastline was affected by erosion which was strong around the main river mouths, due to numerous hydraulic dams which reduced the sediment supply. Nowadays, the coast is rather stable and only the Sele mouth

zone is in erosion (Alberico et al. (2012)). The wave climate was obtained by a directional waverider wave buoy (40°27'26.4"N, 14°51'41.16"E) installed and managed by the Provincial Authority in the Bay of Salerno on approx. 35 meter deep water, for 2014-2016 years. The directional distribution of the significant wave heights, consisting of 32024 samples (Fig. 1b), is in close agreement with the one obtained by the longer data set of the offshore buoy of Ponza (Piscopia et al. (2002)). Figure 1c gives the same directional distribution for significant wave heights $H_s \geq 2$m. Finally, the histogram in Fig. 1d shows the cumulated H_s occurrence frequency for each direction, confirming that the wave directions associated with the most frequent waves are mainly SW (about 56%) and WSW (about 22%).

3 Data and models

3.1 Bathymetric and sediment surveys

We performed two bathymetric surveys along 155 transects spaced by 100 meters, from the dune base till 10m depth. The data acquisition was done using an interferometric sonar single beam system, integrated with the GPS navigation system. All the data obtained from surveys were used to generate a DTM (*Digital Terrain Model*), from which the isobaths needed for detecting rip channels and bars were extracted, with a point density along each transect of two meters. During the first survey 280 sediment samples were also collected, 120 of them in the submerged beach. The analysis of grain size distribution with the Graphic method (Folk and Ward (1957)) was applied, in order to relate the sediment data to morphological ones obtained in other coastal areas (De Pippo et al. (2003); (Pennetta et al., 2016a, b); Mangoni et al. (2016)).

3.2 Sediment dynamical analysis

Submerged beach sediments grain size data was performed in order to carry out the statistical modal analysis. This analysis is based on occurrence frequencies identification related to the most prevalent grain size classes (mode of the grain size distribution), defined as "modal classes", of a single sediment sample. Contours of the modal iso-density were plotted by assigning the proper percentage values of the average modal formula (related to the different modal subpopulations) to sediments samples map points positions. Trend vectors are defined comparing the grain size parameters of each sample with its neighbour, identified on the basis of a characteristic distance that represents the space scale of sampling. Those vectors summarise, in terms of movement directions, the sediment dynamics on the submerged beach of the studied area.

3.3 Wave simulation and hydrodynamic model

In order to simulate the offshore wave features in Gulf of Salerno and propagate them on the coastline, we used a scientific workflow (Giunta et al. (2005)) implemented by the *Campania Center for Marine and Atmospheric Monitoring and Modelling* (CCMMMA) hosted by the University of Naples "*Parthenope*", using a high performance computing (HPC) system (Montella et al. (2011); Di Lauro et al. (2012)) for simulation and open environmental data dissemination (Montella et al. (2007)). The weather/sea forecasting tool has been configured using an HPC infrastructure to manage and run a modeling system based

on the algorithms implemented in the open-source numerical models *Weather Research and Forecasting* (WRF) (Skamarock et al. (2001) and *WaveWatchIII* (WWIII) (Tolman et al. (2009)) organized in a workflow (Pham et al. (2012)). The operational configuration is based on the WRF numerical model (Zinzi et al. (2012)) which gives the atmospheric forcing (10 meters wind fields) needed to estimate the offshore waves. Wave simulations were carried out using the *WaveWatch* III, a third generation wave model developed at NOAA/NCEP. Preliminary implementation and validation for simulating the wave propagation along the Campania Region coastline (Gulf of Naples) were conducted by Benassai and Ascione (2006). Subsequently WRF and WWIII models were coupled in an operational configuration for realtime applications, using also a high resolution bathymetry, to simulate extreme weather coastal floodings along the coast of the municipality of Naples ((Di Luccio et al., 2015, 2016)). The WRF model domain has been configured with 350x200 grid points and 0.01° spatial resolution in latitude (Lat_{min}=39.50N, Lat_{max}=41.49N) and in longitude (Lon_{min}=12.50E, Lon_{max}=15.99E), covering the South Tyrrhenian Sea. WWIII model outputs include gridded fields with the associated significant wave heights (H_s), periods (T_m), directions (Dir) and relative spectral informations.

The offshore wave model outputs were the forcing of the 2D near-shore model XBeach (Roelvink, 2010). This is a two-dimensional model for wave propagation, long waves and mean flow, sediment transport and morphological beach changes during storms. XBeach concurrently solves the time-dependent short wave action balance, roller energy equations, nonlinear shallow water equations of mass and momentum, sediment transport formulations and the bed update on the scale of wave groups. In the Netherlands, a rip current prediction model system was used on the basis of bathymetry measurement through the application application of the XBeach hydrodynamic model (Roelvink et al. (2009)). In this paper XBeach was used to confirm, through hydrodynamic simulations, the occurrence of bathymetric rips evidence by the rip channels previously identified. For this purpose, the model was run with the offshore wave conditions identified in the month of February 2008, obtained by the WWIII wave model. The computational grid has generated merging field data collected in 2008 and the deeper bathymetry, from 10m to 40m depth, supplied by the Istituto Idrografico della Marina Italiana. An irregular mesh was used to obtain a higher resolution across the surf zone and a lower resolution far from the coast. The size of the elements was about 5m on the beach and 25m off the coast. The wave conditions at the offshore boundary were inserted using the JONSWAP spectrum module using the wave condition supplied by WWIII model for rip currents events highlighted by sediment transport vectors in 2008.

3.4 UAV survey

An UAV (*Unmanned aerial vehicle*) hexacopter was used for rip current observations (Fig. 2a, b, c). The UAV weighed about 2500g, carried on board a GPS, a multi-directional accelerometer and a remote flight control. The max height and max radius (vertical and horizontal distance between the aircraft and the home point) were set to the default value of 2000m. The hovering accuracy was ±0.8m in vertical and ±2.5m in horizontal, while the max ascent and descent speed were 6m/s and 4.5 m/s, respectively. A failsafe function system was activated if the connection between the multirotor and the remote control was accidentally disconnected during flight, which provided fly back to the point of take-off and land automatically. The UAV was equipped with a Canon ELPH 130 camera with 16 Mpixel (4608 by 3456 pixels) sensor because of its lightweight, manual

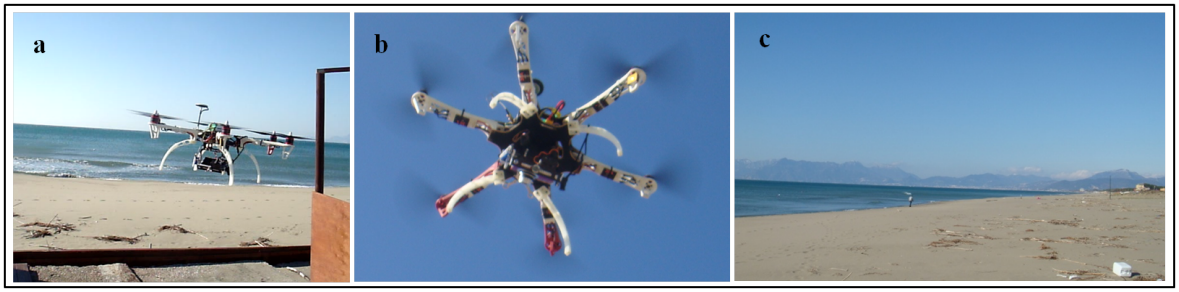

Figure 2. UAV on flight on the surveyed beach.

functions, and programming capabilities through open source custom software. Prior to the survey for the case study, a team deployed georeferenced mobile targets as ground control points (GCP) in the ground using the Trimble R6 DGPS (*Differential Global Positioning System*) in RTK mode. Some targets (297mm×240mm) were placed between the coastline and the upper beach to georeference the UAV acquisition, necessary to spatially compare the different shots.

4 Results

4.1 Sediment analysis and morphodynamics

Comparison of different profiles is used to make morphodynamic characterization on the study area. The bathymetric difference between DTM recorded in February and September 2008 was mapped with a resolution of 5x5 m^2, with the areas suffering from a bathymetric drop of more than 0.1m (reduction of sediment volumes), the ones characterized by a bathymetric lifting of more than 0.1m (increased sediment volumes) and the areas remaining substantially in equilibrium, with the difference in height between -0.1m and +0.1m (Fig. 3a, with the detail north of the Sele mouth in Fig. 3b). The comparison between the two morphological structures derived from the different bathymetric surveys showed the formation of transverse channels to the coast, engraved at the bottom, probably generated by rip currents. These channels are developed mainly between 0 and 5 meters affecting the bars, in origin parallel to the shore, fragmenting them into smaller sand bars, transverse to the shoreline. The bars are constituted by fine and relatively unsorted sands. The increased size of the sediment in the channels as well as its higher sorter correlates well with the high hydrodynamic energy of flowing water in the channels modeled by rip currents.

4.2 Hydrodynamics

The results of the offshore wave numerical simulations and propagation on shoaling waters have been used to establish the inshore wave conditions which are responsible for the sediment transport behaviour. In particular, the waves coming offshore from WSW, which occur with almost 20% percentage, due to a significant clockwise rotation in the shoaling zone, giving rise to waves almost normal to the bathymetry. The wave normal incidence is responsible for the coastal cell circulation and the associated rip currents (Fig. 4a). The waves coming offshore from SW, which occur with almost 58% also show a similar

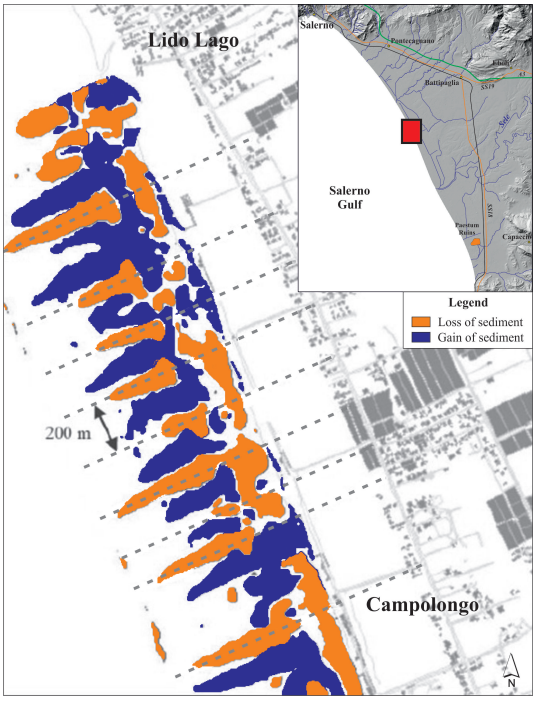

Figure 3. Loss and gain of sediment volumes in the north of the Sele mouth (modified from Pennetta et al. (2011b)). The dotted lines representing the rip channels identifying the most probable position of the rip currents.

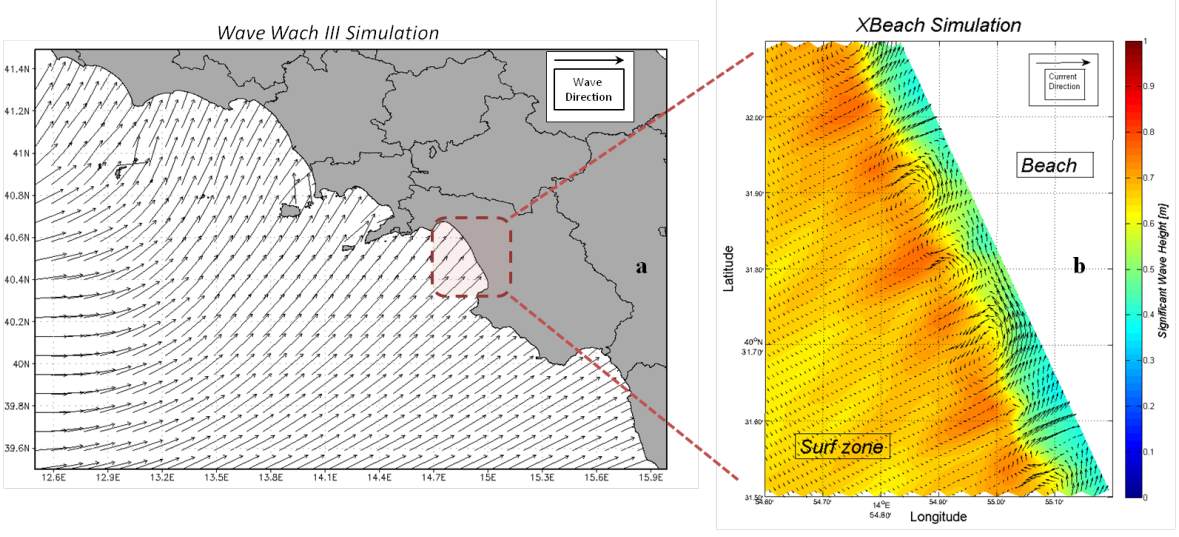

Figure 4. Offshore wave simulation associated with bathymetric survey of February 2008 with wave direction coming from WSW (a); Hydrodynamic wave simulation giving rise to rip current formation (b)).

behaviour, giving rise to the same cell circulation. Nevertheless, the frequency distributions of the highest waves shows the more significant influence of the western waves, which are susceptible to generate an almost longshore transport coming from NW.

The XBeach model output reproduced the rip currents analysed with sediment transport vectors (Fig. 4b). The results describe the wave height incidence and the flow direction simulated by XBeach model, at 16:00 PM of February 2, 2008. In particular, four rip-current cells are evident in the simulations, as well as a significant current flow directed towards offshore the rip spacing which is consistent with the results obtained by the bathymetric comparison. Moreover, the results show the rotation of the flow close to the coastline during the time step considered, and the decrease of the wave height in the rip neck in comparison with the feeder current zone. These results show that the rip current flows do not occur during extreme events, rather confirm that they occur when the significant wave height (H_s) values are between 0.5m and 1m, with mean wave periods (T_m) between 4 and 6 seconds. The simulations also put the emphasis on the fact that cell circulation is driven by longshore gradients in wave set-up and beach morphology.

4.3 Transport trends

The procedure proposed by Gao and Collins (1994) defined trend vectors for the 120 sampling considered. According to this procedure, five grain size trends were associated with net transport directions, reported in table 1 together with their percentage of occurrence. Coarse sand (SP2) with a frequency of 21.76%, Medium sand (SP3) with a frequency of occurrence of 25.45%, Fine sand (SP4) with a frequency of occurrence 20.08% and Very Fine Sand (SP5) with a frequency of occurrence of 30.66%, were the most statistically significant classes for the sediment transport vectors identification. The first was allocated more or less in a uniform way, between foreshore and the depth of -2m, the second showed a spot pattern between foreshore and the depth of -3m. The third is confined to a wide zone of the submerged beach, the last one is located all over the submerged beach with a modal frequency gradient following the bathymetry patterns towards the open sea (according to the typical behaviour of the lower grain size particles). This very fine sand modal fraction SP5 was mostly associated with the rip currents, evidenced by well-defined sediment transport vectors patterns, with moving directions (perpendicular to the shoreline) towards the open sea (Fig. 5a). The modal subpopulation SP4 (Fine Sand), showed a more complex coastal dynamics (Fig. 5b). This grain size fraction seemed to move, driven by rip currents, towards open sea only within the -3/-4m depths, then the sediments have shown to rotate and run parallel to the shoreline mainly South-eastwards, driven by longshore currents.

4.4 Google Earth™ products and UAV survey

The rip current features obtained by the hydrodynamic and sediment calculations were compared with the ones observed by Google Earth™ (Fig. 6a,b,c) and UAV images (Fig. 7a,b,c,d,e). corresponding with the sea states characteristics reported in table 2. The comparison between the simulated and remotely observed sea states evidences that the simulated sea states coming from W correspond to the ones observed on 28/06/2007 and 02/05/2013 (Fig. 6a, b), while the ones coming from WSW correspond to the sea states observed on 29/05/2015 (Fig. 6c). Finally, the UAV observed rip currents are associated with sea states being characterized by longer swell mixed with sea waves generated by wind directions coming from land.

Table 1. Frequency distribution for each modal class of the sample

	Modal class	Size range [mm]	Modal peak [mm]	Frequency [%]
SP1	GRAVEL	19.214-2.378	2.378	2.06
SP2	COARSE SAND	0.802 -0.595	0.595	21.76
SP3	MEDIUM SAND	0.296-0.254	0.294	25.45
SP4	FINE SAND	0.250-0.210	0.213	20.08
SP5	VERY FINE SAND	0.105-0.101	0.102	30.66

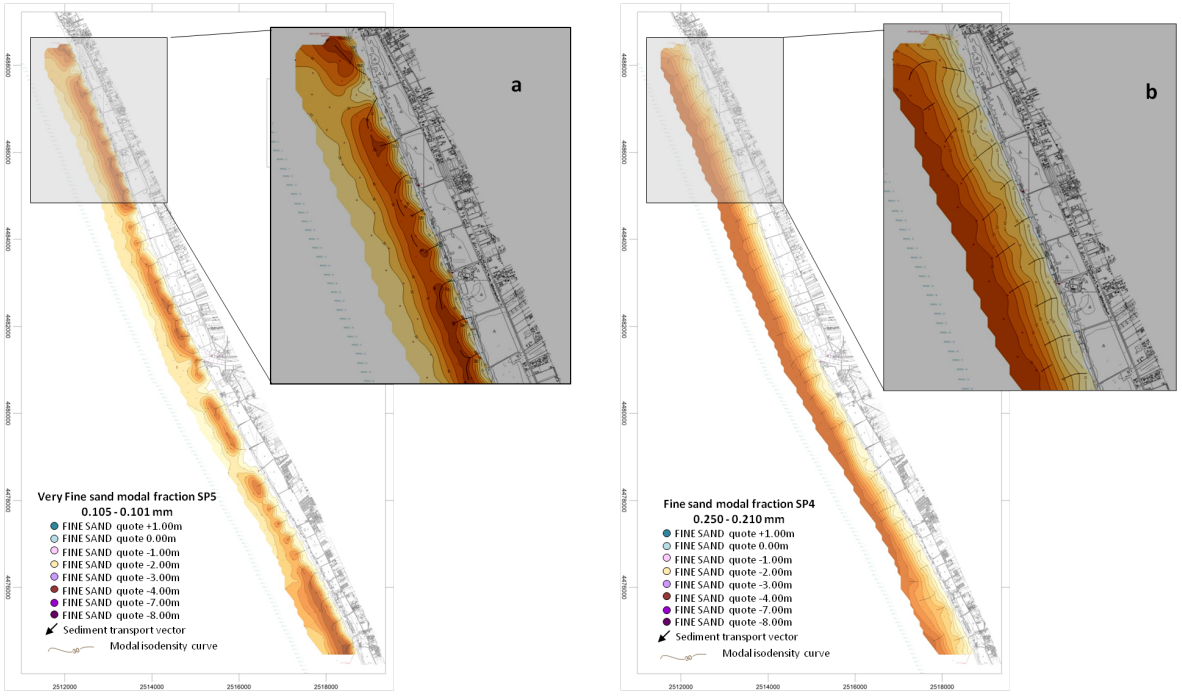

Figure 5. Sediment transport vectors for the whole area referred to the modal subpopulation SP5-Very Fine Sand (a) and SP4-Fine Sand(b).

This residual swell coming from W and SW is already capable of giving rise to low-defined rip currents, as shown in Fig. 7. These qualitative results are confirmed by the values of the non-dimensional fall velocity Ω given for each transect and for each observed period in the histogram of Fig. 8. The results show clearly that i) the mean Ω values are quite different for the period in which well defined rip-currents are observed and periods associated with low defined rips and ii) the mean Ω values associated with the sea states of 2013 and 2015 (well defined rip-currents) are included in the range reported by Castelle et al. (2010), while the values associated with the first and last observation period (2007 and 2017) are outside of this range.

Figure 6. Evidence of rip-currents in Google Earth™ images a) 28/06/2007 (Image©2016 European Space Imaging); b) 02/05/2013 (Image©2016 Digital Globe); c) 29/05/2015 (Image Landsat/Copernicus).

Table 2. Wave characteristics during numerical simulations and remote observations

	28/06/2007	02/02/2008	02/05/2013	29/05/2015	21/01/2017
H_s [m]	1.46	0.91	0.33	0.46	0.67
T_m [sec]	5.8	4.11	2.99	3.47	2.71
Dir [°N]	275.10	228.29	284.23	206.20	14.83

5 Discussion

Comparison of different profiles and wave numerical simulations in the shallow coastal area of the Sele mouth in the Gulf of Salerno (Southern Italy) identified the features of the near shore circulation, which often produced bathymetric rip currents. The hydrodynamic inshore simulations identified clearly the cell circulation that is associated with the shore-normal wave propagation evidenced by the WWIII model. These hydrodynamic results are in agreement with the sediment transport trends, which evidenced that the class of fine sand is brought into suspension in a wide zone of the submerged beach between the -2m and -7m bathymetry, giving rise to rip currents for the first 2-3m depth, then being distributed by the longshore coastal dynamics. The rip spacing of few hundred meters obtained by the bathymetric, sediment and hydrodynamic annalysis is in accordance with Wright and Short (1984).

6 Conclusions

In this paper the rip current morphodynamics on a micro-tidal beach addressed by means of hydrodynamic and sediment dynamics modelling was validated by Google Earth™ and UAV observations. The wave numerical simulations identified the occurrence of a rip current cell circulation, both in terms of heights, periods and directions. These hydrodynamic conditions,

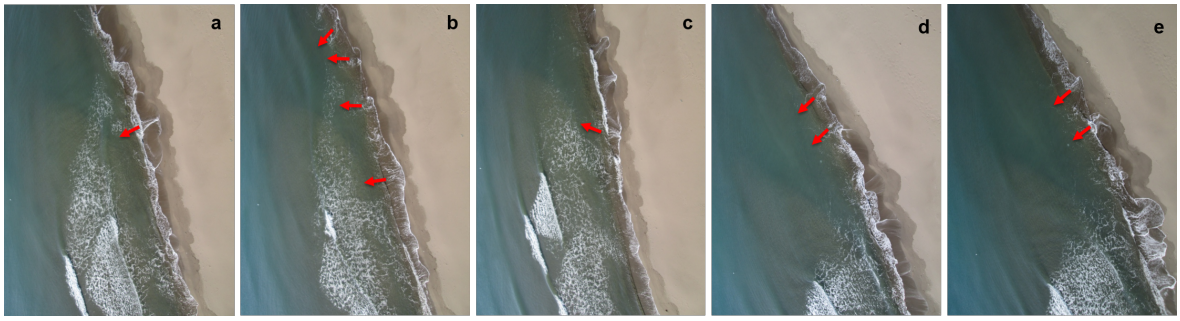

Figure 7. Evidence of rip-currents during UAV acquisition in individual images captured on 21/01/2017. The red arrows are representative of the rip-currents.

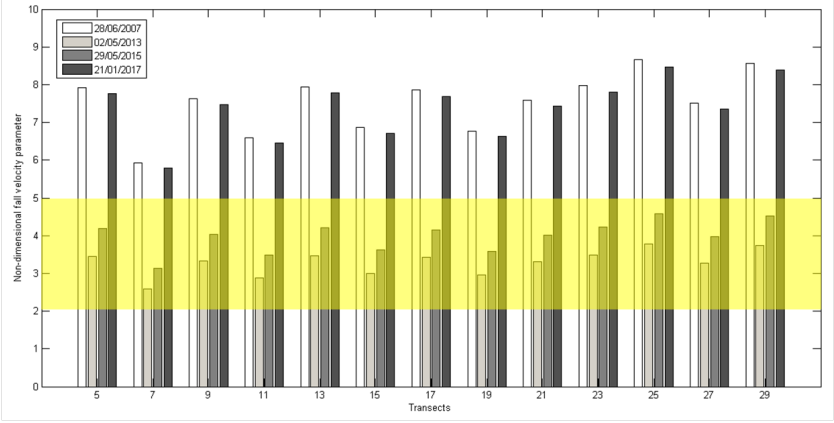

Figure 8. Histogram of the Ω values of each transect. The yellow strip is the range mostly associated with rip currents (Castelle et al. (2010)).

together with the sediment characteristics, were related with the non-dimensional fall velocity parameter, which proved to be an efficient index for the rip current formation. In fact, the remote observations of well-defined rips performed by Google Earth^{TM} images and UAV confirmed the rip current occurrence in a restricted Ω range. The present results can be used as a basis for a beach hazard forecasting system in order to enhance the swimmers safety. As a matter of fact, the observed channel rips are quite stationary over several days in this long stretch of coastline, giving rise to persistent danger in the surf zone.

Acknowledgements. The authors are grateful to the CCMMMA (*Centro Campano per il Monitoraggio e la Modellistica Marina e Atmosferica*, http://meteo.uniparthenope.it) that is the forecast service of the University of Napoli "*Parthenope*" for the real time monitoring and forecast of marine, weather and air quality conditions in the Mediterranean area, with a specific focus on the Campania Region. The CCMMMA provided the hardware and software resources for the offshore numerical simulations. Additional thanks are addressed to the C.U.G.RI. (*Inter-University Consortium for the Prediction and Prevention of Major Hazards*), to the Civil Protection Department of the Campania Region which provided the Salerno wave buoy data, and to Dr. Caira who provided the UAV survey on the coastal area.

References

Alberico, I., Amato, V., Aucelli, P., D'argenio, B., Di Paola, G., and Pappone, G.: Historical shoreline change of the Sele Plain (Southern Italy): The 1870–2009 time window, Journal of Coastal Research, 28, 1638–1647, 2012.

Amato, V., Aucelli, P., Ciampo, G., Cinque, A., Di Donato, V., Pappone, G., Petrosino, P., Romano, P., Rosskopf, C., and Ermolli, E. R.: Relative sea level changes and paleogeographical evolution of the southern Sele plain (Italy) during the Holocene, Quaternary International, 288, 112–128, 2013.

Aucelli, P. P., Amato, V., Budillon, F., Senatore, M. R., Amodio, S., D'Amico, C., Da Prato, S., Ferraro, L., Pappone, G., and Ermolli, E. R.: Evolution of the Sele River coastal plain (southern Italy) during the Late Quaternary by inland and offshore stratigraphical analyses, Rendiconti Lincei, 23, 81–102, 2012.

Bartole, R., Savelli, D., Tramontana, M., and Wezel, F.-C.: Structural and sedimentary features in the Tyrrhenian margin off Campania, Southern Italy, Marine Geology, 55, 163–180, 1984.

Benassai, G. and Ascione, I.: Implementation and validation of WaveWatchIII model offshore the coastlines of Southern Italy, in: 25th International Conference on Offshore Mechanics and Arctic Engineering, pp. 553–560, American Society of Mechanical Engineers, 2006.

Benassai, G., Di Paola, G., and Aucelli, P.: Coastal risk assessment of a micro-tidal littoral plain in response to sea level rise, Ocean & Coastal Management, 104, 22–35, 2015.

Bowen, A. J.: Rip currents: 1. Theoretical investigations, Journal of Geophysical Research, 74, 5467–5478, 1969.

Brander, R., Dominey-Howes, D., Champion, C., Del Vecchio, O., and Brighton, B.: Brief communication: a new perspective on the Australian rip current hazard, Natural hazards and earth system sciences, 13, 1687, 2013.

Brighton, B., Sherker, S., Brander, R., Thompson, M., and Bradstreet, A.: Rip current related drowning deaths and rescues in Australia 2004-2011, Natural hazards and earth system sciences, 13, 1069, 2013.

Casciello, E., Cesarano, M., and Pappone, G.: Extensional detachment faulting on the Tyrrhenian margin of the southern Apennines contractional belt (Italy), Journal of the Geological Society, 163, 617–629, 2006.

Castelle, B., Michallet, H., Marieu, V., Leckler, F., Dubardier, B., Lambert, A., Berni, C., Bonneton, P., Barthelemy, E., and Bouchette, F.: Laboratory experiment on rip current circulations over a moveable bed: Drifter measurements, Journal of Geophysical Research: Oceans, 115, 2010.

De Pippo, T., Donadio, C., and Pennetta, M.: Morphological control on sediment dispersal along the southern Tyrrhenian coastal zones (Italy), Geol Rom, 37, 113–121, 2003.

Di Lauro, R., Giannone, F., Ambrosio, L., and Montella, R.: Virtualizing general purpose GPUs for high performance cloud computing: an application to a fluid simulator, in: 2012 IEEE 10th International Symposium on Parallel and Distributed Processing with Applications, pp. 863–864, IEEE, 2012.

Di Luccio, D., Budillon, G., Montella, R., Pugliese Carratelli, E., and Dentale, F.: Progettazione e implementazione di un sistema di allerta inindazione per le coste del Comune di Napoli, in: Aiello, G. and Sorgente, R., Oceanografia operaTiva e Tecnologie Informatiche per la sicurezza Marittima, pp. 48–54, 2015.

Di Luccio, D., Benassai, G., Budillon, G., Di Leo, A., Montella, R., Pugliese Carratelli, E., and Reale, F.: Operational modeling issues in extreme weather coastal flooding, in: Book of Abstracts of 8th International Workshop on Modeling the Ocean (IWMO), p. 61, 2016.

Di Paola, G., Iglesias, J., Rodríguez, G., Benassai, G., Aucelli, P., and Pappone, G.: Estimating coastal vulnerability in a meso-tidal beach by means of quantitative and semi-quantitative methodologies, Journal of Coastal Research, pp. 303–308, 2011.

Di Paola, G., Aucelli, P. P., Benassai, G., and Rodríguez, G.: Coastal vulnerability to wave storms of Sele littoral plain (southern Italy), Natural hazards, 71, 1795–1819, 2014.

Drozdzewski, D., Shaw, W., Dominey-Howes, D., Brander, R., Walton, T., Gero, A., Sherker, S., Goff, J., and Edwick, B.: Surveying rip current survivors: preliminary insights into the experiences of being caught in rip currents, Natural Hazards and Earth System Sciences, 12, 1201, 2012.

Folk, R. L. and Ward, W. C.: Brazos River bar: a study in the significance of grain size parameters, Journal of Sedimentary Research, 27, 1957.

Gao, S. and Collins, M.: Analysis of grain size trends, for defining sediment transport pathways in marine environments, Journal of Coastal Research, pp. 70–78, 1994.

Giunta, G., Montella, R., Mariani, P., and Riccio, A.: Modeling and computational issues for air/water quality problems: A grid computing approach, Nuovo Cimento C Geophysics Space Physics C, 28, 215, 2005.

Holman, R. A., Brodie, K. L., and Spore, N. J.: Surf Zone Characterization Using a Small Quadcopter: Technical Issues and Procedures, IEEE Transactions on Geoscience and Remote Sensing, 2017.

Longuet-Higgins, M. S. and Stewart, R.: Radiation stresses in water waves; a physical discussion, with applications, in: Deep Sea Research and Oceanographic Abstracts, vol. 11, pp. 529–562, Elsevier, 1964.

MacMahan, J. H., Thornton, E. B., and Reniers, A. J.: Rip current review, Coastal Engineering, 53, 191–208, 2006.

Mangoni, O., Aiello, G., Balbi, S., Barra, D., Bolinesi, F., Donadio, C., Ferrara, L., Guida, M., Parisi, R., Pennetta, M., et al.: A multidisciplinary approach for the characterization of the coastal marine ecosystems of Monte Di Procida (Campania, Italy), Marine Pollution Bulletin, 112, 443–451, 2016.

Montella, R., Giunta, G., and Riccio, A.: Using grid computing based components in on demand environmental data delivery, in: Proceedings of the second workshop on Use of P2P, GRID and agents for the development of content networks, pp. 81–86, ACM, 2007.

Montella, R., Coviello, G., Giunta, G., Laccetti, G., Isaila, F., and Blas, J. G.: A general-purpose virtualization service for HPC on cloud computing: an application to GPUs, in: International Conference on Parallel Processing and Applied Mathematics, pp. 740–749, Springer, 2011.

Pappone, G., Alberico, I., Amato, V., Aucelli, P., and Di Paola, G.: Recent evolution and the present-day conditions of the Campanian Coastal plains (South Italy): the case history of the Sele River Coastal plain, WIT Trans Ecol Environ, 149, 15–27, 2011.

Pappone, G., Aucelli, P. P. C., Aberico, I., Amato, V., Antonioli, F., Cesarano, M., Di Paola, G., and Pelosi, N.: Relative sea-level rise and marine erosion and inundation in the Sele river coastal plain (Southern Italy): scenarios for the next century, Rendiconti Lincei, 23, 121–129, 2012.

Pennetta, M., Corbelli, V., Esposito, P., Gattullo, V., and Nappi, R.: Environmental Impact of Coastal Dunes in the Area Located to the Left of the Garigliano River Mouth (Campany, Italy)., Journal of Coastal Research, pp. 421–427, 2011a.

Pennetta, M., Sica, M., and Abbundo, R.: Canali da rip currents nella spiaggia sommersa presso la foce del Fiume Sele (Golfo di Salerno, Italia), in: Congresso annualeGEOSED, pp. 27–28, 2011b.

Pennetta, M., Brancato, V. M., De Muro, S., Gioia, D., Kalb, C., Stanislao, C., Valente, A., and Donadio, C.: Morpho-sedimentary features and sediment transport model of the submerged beach of the 'Pineta della foce del Garigliano'SCI Site (Caserta, southern Italy), Journal of Maps, 12, 139–146, 2016a.

Pennetta, M., Stanislao, C., D'Ambrosio, V., Marchese, F., Minopoli, C., Trocciola, A., Valente, R., and Donadio, C.: Geomorphological features of the archaeological marine area of Sinuessa in Campania, southern Italy, Quaternary International, 425, 198–213, 2016b.

Pham, Q., Malik, T., Foster, I. T., Di Lauro, R., and Montella, R.: SOLE: Linking Research Papers with Science Objects., in: IPAW, pp. 203–208, Springer, 2012.

Piscopia, R., Inghilesi, R., Panizzo, A., Corsini, S., and Franco, L.: Analysis of 12-year wave measurements by the Italian Wave Network, in: 28° ICCE Conference, pp. 121–133, 2002.

Roelvink, D., Reniers, A., Van Dongeren, A., de Vries, J. v. T., McCall, R., and Lescinski, J.: Modelling storm impacts on beaches, dunes and barrier islands, Coastal engineering, 56, 1133–1152, 2009.

Short, A. D. and Brander, R. W.: Regional variations in rip density, Journal of Coastal Research, pp. 813–822, 1999.

Skamarock, W. C., Klemp, J. B., and Dudhia, J.: Prototypes for the WRF (Weather Research and Forecasting) model, in: Preprints, Ninth Conf. Mesoscale Processes, J11–J15, Amer. Meteorol. Soc., Fort Lauderdale, FL, 2001.

Tolman, H. L. et al.: User manual and system documentation of WAVEWATCH III TM version 3.14, Technical note, MMAB Contribution, 276, 220, 2009.

Turner, I. L., Harley, M. D., and Drummond, C. D.: UAVs for coastal surveying, Coastal Engineering, 114, 19–24, 2016.

Wright, L. and Short, A. D.: Morphodynamic variability of surf zones and beaches: a synthesis, Marine geology, 56, 93–118, 1984.

Zhang, Z., Li, N., Xie, W., Liu, Y., Feng, J., Chen, X., and Liu, L.: Assessment of ripple effect and spatial heterogeneity of total losses in the capital of China after a great catastrophe shocks, Natural hazards and earth system sciences, 2012.

Zinzi, A., Montella, R., Agrillo, G., Riccio, A., and Budillon, G.: Validation of the Uniparthenope ARW-WRF Model for a Convective Case Study, in: Book of Abstracts of 92nd American Meteorological Society Annual Meeting, 2012.